British Journal of Clinical Pharmacology

Br J Clin Pharmacol (2019) **85** 626–633 626

ORIGINAL ARTICLE

Population pharmacokinetics of oral ivermectin in venous plasma and dried blood spots in healthy volunteers

Correspondence Felix Hammann, Division of Clinical Pharmacology & Toxicology, University Hospital Basel, Switzerland. Tel.: +41 61 328 6847; Fax: +41 61 265 4560; E-mail: felix.hammann@unibas.ch

Received 23 August 2018; **Revised** 23 November 2018; **Accepted** 29 November 2018

Urs Duthaler[1,2], Claudia Suenderhauf[1,2], Mats O. Karlsson[3], Janine Hussner[4], Henriette Meyer zu Schwabedissen[4], Stephan Krähenbühl[1,2] and Felix Hammann[1,2,3]

[1]Division of Clinical Pharmacology & Toxicology, University Hospital Basel, Switzerland, [2]Department of Biomedicine, University of Basel, Switzerland, [3]Department of Pharmaceutical Biosciences, Uppsala University, Uppsala, Sweden, and [4]Biopharmacy, Department of Pharmaceutical Sciences, University of Basel, Basel, Switzerland

Keywords Drug analysis, parasitology < Infectious diseases, pharmacokinetics, pharmacometrics, tropical diseases < Infectious diseases

AIMS

The anthelminthic ivermectin is receiving new attention as it is being repurposed for new indications such as mass drug administrations for the treatment of scabies or in malaria vector control. As its pharmacokinetics are still poorly understood, we aimed to characterize the population pharmacokinetics of ivermectin in plasma and dried blood spots (DBS), a sampling method better suited to field trials, with special focus on the influence of body composition and enterohepatic circulation.

METHODS

We performed a clinical trial in 12 healthy volunteers who each received a single oral dose of 12 mg ivermectin, and collected peripheral venous and capillary DBS samples. We determined ivermectin concentrations in plasma and DBS by liquid chromatography tandem mass spectrometry using a fully automated and scalable extraction system for DBS sample processing. Pharmacokinetic data were analysed using non-linear mixed effects modelling.

RESULTS

A two-compartment model with a transit absorption model, first-order elimination, and weight as an influential covariate on central volume of distribution and clearance best described the data. The model estimates (inter-individual variability) for a 70 kg subject were: apparent population clearance 7.7 (25%) l h^{-1}, and central and peripheral volumes of distribution 89 (10%) l and 234 (20%) l, respectively. Concentrations obtained from DBS samples were strongly linearly correlated (R^2 = 0.97) with plasma concentrations, and on average 30% lower.

CONCLUSION

The model accurately depicts population pharmacokinetics of plasma and DBS concentrations over time for oral ivermectin. The proposed analytical workflow is scalable and applicable to the requirements of mass drug administrations.

DOI:10.1111/bcp.13840

WHAT IS ALREADY KNOWN ABOUT THIS SUBJECT

- Ivermectin shows great pharmacokinetic variability after oral administration, some of which has been attributed to enterohepatic circulation.
- New indications for ivermectin that are currently being pursued include mass drug administrations in scabies or malaria vector control, for which dried blood spots (DBS) could be a practicable blood sampling method.

WHAT THIS STUDY ADDS

- Enterohepatic circulation does not seem to influence ivermectin pharmacokinetics in healthy volunteers.
- Besides weight, no other measured physiological covariates such as body fat showed any effects on ivermectin pharmacokinetics.
- Automated DBS analysis is a feasible and scalable approach to monitor ivermectin exposure in field trials.

Introduction

Ivermectin is an antiparasitic agent registered for human use in the 1980s. It is a derivative of avermectin B1 and is formulated as an 80:20 mixture of 22,23-dehydro-B1a and B1b. In invertebrates such as helminths, ivermectin inhibits synaptic transmission by binding to glutamate-gated chloride channels (GluCl) in nerve and muscle tissue. This results in neuronal hyperpolarization, paralysis and, eventually, death [1]. Vertebrates express different members of the Cys-loop family of ligand-gated ion channels with which ivermectin can also interact and which can lead, for instance, to neurotoxicity [2]. Overall, ivermectin is considered to have an excellent safety profile [3]. Ivermectin has been used in more than 2.7 billion individuals over the last three decades for the control of river blindness (onchocerciasis), lymphatic filariasis and other neglected tropical diseases [4]. Demand for ivermectin is expected to increase in the coming years due to new indications being pursued including, for instance, mass drug administrations (MDAs) for the treatment of scabies and malaria [1, 5, 6].

Despite its widespread use, the pharmacokinetic (PK) characteristics of ivermectin are still poorly understood. The sources of pharmacokinetic variability, including the proposed existence of enterohepatic circulation (EHC), have been reviewed before [1, 6, 7]. Previous PK studies employed one- or two-compartment models with first-order oral absorption to describe the pharmacokinetics of ivermectin [8, 9]. There have been two prior population-based PK studies of ivermectin, both of which were re-analyses of interaction trials involving ivermectin. The first was a re-analysis of an interaction study with azithromycin using a two-compartment model with first-order oral absorption and elimination, and additionally implementing a mixture model for bioavailability [10]. The second, a 2017 study with pooled data from a 2006 trial in healthy Thai volunteers with albendazole +/− praziquantel as concomitant medications, also employed a two-compartment model with linear elimination, but had two transit absorption compartments [11, 12].

In the current work, we investigated the oral pharmacokinetics of ivermectin with special focus on body composition and enterohepatic circulation. We also evaluated the utility of dried blood spots (DBS), a micro-sampling technique that requires less than 20 µl of capillary whole blood (compared to 2–4 ml in conventional venipuncture), which makes this technique attractive for PK studies in children. Moreover, DBS samples do not require centrifugation and can be transported at room temperature, which facilitates blood sampling in field studies. In order to understand the variability in pharmacokinetics of ivermectin, we developed a population-pharmacokinetic model with additional focus on body composition and enterohepatic circulation, which also relates the concentrations in plasma to those obtained from DBS for possible future use in the interpretation of results from field trials.

Methods

Clinical trial

Ethical considerations. The Ethical Committee of Northwestern and Central Switzerland (EKNZ, reference number: 2016-01060) and the Swiss Agency for Therapeutic Products (Swissmedic, reference number: 2016DR1156) approved this study. It is registered at ClinicalTrials.gov with the identifier NCT02963324. The study was conducted in accordance with the Declaration of Helsinki and International Conference on Harmonization Guidelines in Good Clinical Practice. Randomized volunteers received financial compensation for their participation in the trial.

Trial design and study procedures. The trial was a single-centre, single-dose and open-label study conducted at the University Hospital Basel, Switzerland. Written informed consent was obtained from all participants prior to enrolment procedures.

Both male and female subjects were eligible for the study. Inclusion criteria were an age of 18–65 years, a body mass index (BMI) of 18–30 kg m^{-2}, body weight ≥ 50 kg, and good health as assessed by medical history, physical examination, and laboratory analyses. Exclusion criteria were history or presence of hepato-biliary or gastrointestinal disease, psychiatric pathology, drug or alcohol abuse, allergic conditions relevant to the trial, and the intake of medication that could interfere with the trial [in particular substances that could interact with cytochrome P_{450} (CYP3A4) or **P-glycoprotein** (P-gp, MDR1, ABCB1)]. On the day of screening, we also performed abdominal sonography to measure volumes of the liver, the gallbladder and the kidneys [13–15]. All subjects received genotyping for an MDR1 polymorphism (MDR1 3435C>T, rs1045642), which has been associated with lower P-gp expression, and altered bioavailability of substrate drugs, like ivermectin [16, 17]. Lastly, volunteers underwent anthropometric measurements, which consisted of skinfold

caliper measurements at four sites (biceps, triceps, subscapular, iliac crest skinfolds) according to the Durnin–Womersley method to calculate body fat percentages (BF%) using Siri's equation [18, 19]. Additionally, we used a commercially available body impedance analysis scale (Tanita BC-601 Segmental Body Composition Monitor, Tanita Europe BV, Amsterdam, The Netherlands) to obtain lean body mass, total body water (TBW), and another estimation of BF%.

On Day 1, subjects arrived at the trial site in a fasted state. Thirty minutes before dosing, subjects were given a high-fat breakfast, and at 5 h post-dose they received a high-fat lunch to stimulate gallbladder emptying. During their stay at the study site on Day 1, subjects were not allowed to consume anything else but water and the meals provided. All subjects were given a single dose of oral ivermectin 12 mg (4 tablets Stromectol® 3 mg, MSD France, 92 418 Courbevoie Cedex, France), remained at the site until 12 h post dose for surveillance and sampling, and returned for additional sampling on Days 2 and 3. We obtained peripheral venous blood samples prior to dosing, and at 1, 2, 3, 4, 5, 6, 7, 8, 9, 10, 11, 12, 24, 36, 48 and 72 h post dose, and centrifuged them immediately after drawing. We took DBS samples from subjects' fingertips prior to dosing, and at 2, 4, 6, 8, 12, 24, 36, 48 and 72 h post dose. These were allowed to dry at ambient temperature, and then were individually packed in plastic bags with silica gel packs. After preparation, biological samples were immediately stored at −20°C before they were transferred to −80°C for permanent storage. Vital signs (blood pressure and heart rate) and adverse events were recorded throughout the study.

Quantification of ivermectin

Ivermectin was analysed by liquid chromatography (Shimadzu, Kyoto, Japan) tandem mass spectrometry (API 5500 Qtrap, ABSciex, MA, USA). In brief, a Kinetex C8 (2.6 µm, 100 Å, 50 × 2.1 mm) analytical column (Phenomenex, Torrance, USA) was used for the chromatography of ivermectin. The mobile phases were 20 mM ammonium formate (mobile A) and methanol (mobile B) both supplemented with 0.1% formic acid. The following gradient programme was used: 0–0.25 min 2% mobile B, 0.75 min 75% mobile B, 2.5–3.25 min 95% mobile B, and 3.25–3.75 min 2%. The flow rate was 0.6 ml min^{-1} and the separation was performed at 50°C. The applied gradient resulted in a retention time of 1.9 min. Ivermectin and ivermectin-d2 (internal standard) were analysed by positive electrospray ionization using the mass transitions 892.4 → 569.1 m/z and 895.4 → 571.8 m/z, respectively. Note that the second most abundant mass was used for ivermectin-d2 (877 + 18 (NH_4) m/z: 51.9%).

Plasma samples (50 µl) were extracted with 150 µl IS solution (50 ng ml^{-1} ivermectin-d2 in methanol). The precipitated samples were vortex mixed for 1 min and centrifuged at 10°C and 3220 g for 30 min. Ten microlitres of supernatant was injected into the LC–MS/MS system.

DBS samples were extracted fully automated using a DBS-MS 500 autosampler (CAMAG, Muttenz, Switzerland), which was connected to the LC–MS/MS system. DBS were photographed before and after extraction to exclude inadequate spots. Ten microlitres of internal standard (250 ng ml^{-1} ivermectin-d2 in methanol) were sprayed in a homogeneous layer onto each spot before extracting the DBS at a flow rate of 40 µl min^{-1} with 25 µl of mobile phase A.

Calibrators and quality control samples were prepared in blank human plasma or whole blood, which was spotted onto DBS filter cards (903 grade, Whatman, ME, USA). The chosen calibration range was between 0.5 (lower limit of quantification, LLOQ) to 250 ng ml^{-1} (upper limit of quantification, ULOQ) for plasma and 1 (LLOQ) to 100 ng ml^{-1} (ULOQ) for DBS. QC samples were prepared at low (plasma: 1 ng ml^{-1}, DBS: 2.5 ng ml^{-1}) medium (10 ng ml^{-1}) and high (plasma: 100 ng ml^{-1}, DBS: 50 ng ml^{-1}) concentration levels. An imprecision of less than 15% (LLOQ: 20%) and accuracy between 85 and 115% (LLOQ: 80–120%) was accepted in this study. The signal at the LLOQ was five times higher than the noise signal of blank samples.

Genotyping of rs1045642 (MDR1 3435C>T)

DNA extraction from blood samples was performed as described by the manufacturer using a QiaCube® (Qiagen, Hombrechtikon, Switzerland). Subsequently, DNA content was determined photometrically using a NanoQuant Plate™ and the Tecan Infinite M200 Pro (Tecan, Männedorf, Switzerland). DNA samples were stored at −20°C until further use. Individuals were genotyped by restriction length polymorphism analysis.

Pharmacokinetic modelling

Population pharmacokinetic analysis was carried out using NONMEM (Version 7.4.2; Icon Development Solutions, http://www.iconplc.com, Ellicott City, MD, USA). Data set checkout was performed in Gnu R (Version 3.3.3; R Foundation for Statistical Computing, http://www.R-project.org, Vienna, Austria). Model diagnostic and covariate testing were performed using the Xpose and PsN software packages [20, 21]. The first order conditional estimation with eta-epsilon interaction (*FOCE-I*) was used throughout all runs. We selected models based on goodness-of-fit statistics [e.g. objective function value (minus twice the log-likelihood)], graphical analysis using visual predictive checks (VPCs, n = 1000 simulations), and mechanistic model plausibility. We used non-parametric bootstrap analysis (n = 1000) to assess parameter precisions of the final model.

Model building was done on plasma concentrations first. After the plasma model was completed, we fitted the model simultaneously to plasma and DBS data by adding a correction ratio for DBS samples. We chose this sequential approach because DBS sampling was sparser and not designed to capture the absorption phase and the post-prandial peaks but to compare plasma and DBS levels. As structural models, we tested one-, two- and three-compartment models with first-order elimination. Specifically, we aimed to account for enterohepatic circulation by modelling continuous gallbladder release, single bolus gallbladder release, and gallbladder release controlled by several functions (piecewise switch, sigmoid and sine functions) [22]. We evaluated several different absorption models: first-order absorption with and without lag time, one or more transit compartments, and Weibull-like absorption. For interindividual variability, we assumed log-normal distributions, and we considered additive,

proportional and combined (i.e. additive and proportional) residual error models.

Covariates included in the analysis were age, sex, height, total body weight, BF% (as determined by skinfold-caliper measurements and body impedance analysis), TBW, body surface area (BSA), sonographically determined volumes of gall bladder, liver and kidneys, hematocrit, plasma albumin, and MDR1 3435C>T genotype. After selection of covariates by visual inspection and mechanistic plausibility, we built the covariate model in a stepwise forward addition and backward elimination approach. A decrease in the objective function value (OFV) > 3.84 points (i.e. $P < 0.05$) was the criterion used in forward inclusion of covariates, and an increase in OFV > 6.63 points (i.e. $P < 0.01$) for backward exclusion.

Table 1

Baseline characteristics of the study population

	Median	Range	
Age, years	23	20–36	
Height, cm	173	167–190	
Weight, kg	64.7	57.3–94.2	
Body mass index, kg m^{-2}	21.9	18.1–26.4	
Body surface area, m^2	1.79	1.64–2.22	
Total body water, %	57.1	49.7–64.3	
Body fat (BIA), %	20.5	11.9–31.3	
Body fat (SFC), %	19.5	9.9–33.6	
Gall bladder volume, ml	19.7	12.0–37.7	
Liver volume, ml	1042.2	566.8–1481.4	
Kidney volume, ml	118.9	97.7–164.7	
Hematocrit	0.38	0.37–0.46	
Albumin, g l^{-1}	39.5	35.0–42.0	
Allele frequency	**CC**	**CT**	**TT**
MDR1 C3435T	5 (41.7%)	5 (41.7%)	2 (16.7%)

BIA, body impedance analysis; SFC, skinfold caliper measurements

Table 2

Accuracy and precision data of ivermectin in plasma and DBS samples

Matrix		QC_{Low}	QC_{Mid}	QC_{High}
Plasma	Nominal concentration, ng ml^{-1}	1	10	100
	Calculated concentration, ng ml^{-1}	1.02	10.9	99.7
	Accuracy ± CV, %	102.1 ± 9.7	108.9 ± 2.4	99.7 ± 3.4
	N	4	4	4
DBS	Nominal concentration, ng ml^{-1}	2.5	10	50
	Calculated concentration, ng ml^{-1}	2.27	9.9	47.3
	Accuracy ± CV, %	90.8 ± 3.3	99.0 ± 9.2	94.6 ± 5.1
	N	6	6	6

CV, coefficient of variation (standard deviation, %); QC, quality control sample

Nomenclature of targets and ligands

Key protein targets and ligands in this article are hyperlinked to corresponding entries in http://www.guidetopharmacology.org, the common portal for data from the IUPHAR/BPS Guide to PHARMACOLOGY [23], and are permanently archived in the Concise Guide to PHARMACOLOGY 2017/18 [24].

Results

Clinical trial

Six female and six male healthy volunteers from the region of Basel (Switzerland) were enrolled for the study. There were no screening failures and no dropouts. Baseline demographics and genotyping results are given in Table 1. Overall, volunteers tolerated the drug well, and there were no severe adverse events. Adverse events recorded (number of subjects) included headaches (3), nausea (2), abdominal discomfort (1), diarrhoea (1) and the common cold (2). Gastrointestinal disturbances in particular are known adverse events of ivermectin [25]. Three subjects each had a single asymptomatic hypertensive episode, but targeted questioning revealed that these volunteers had occasionally had similar readings in the past. Individual plasma and DBS concentration profiles are given in the Supporting Information. The two body fat (BF%) methods were in close correlation with each other ($R^2 = 0.89$, slope = 1.04, $P < 0.001$).

Bioanalysis of ivermectin

We collected a total of 119 of 120 planned DBS and 201 of 204 plasma samples (one subject missed a sampling visit, two plasma samples were haemolysed). All DBS samples were taken within 15 min after the peripheral venous sampling. Calibration lines were linear with a correlation coefficient (R) of more than 0.995. Accuracy and precision data are summarized in Table 2. The precision was <9.7% and accuracy between 90.8 and 108.9%, which is in line with regulatory guidelines for bioanalytical methods [26]. Overall, there was a strong linear correlation between the two sampling techniques, with DBS concentrations being about 30% lower than the corresponding plasma concentrations ($R^2 = 0.97$, slope = 0.75, intercept = −0.74). Bland–Altman plots are given in the Supporting Information as Figure S1 (%Difference Plasma

to DBS: +34%, 95% limits of agreement: +12% to +56%). The agreement between plasma and DBS did not show a trend across the measured concentrations (Figure S2).

Pharmacokinetic analysis

After exclusion of two plasma samples that had been drawn incorrectly, a total of 294 post-dose measurements from 12 patients were used for analysis. All of these were above the LLOQ. We settled on a two-compartment model with first-order elimination, with a chain of transit compartments to model absorption (fixed to six), and a combined additive and proportional residual error model [27]. More complex models were not supported by the data. The structure of the final nonlinear mixed effects model is given in Figure 1. We estimated interindividual variability for clearance (CL/F), volumes of distribution (V_c/F, V_p/F), transfer rates to the peripheral compartment (Q/F), and the mean transit time (MTT) for the absorption compartments. Total body weight was the only covariate that significantly influenced the PK profile of ivermectin. It was introduced into the model in the form of allometric scaling of V_c/F and CL/F with fixed exponents of 1 (V_c/F) and 0.75 (CL/F) for a standardized total body weight of 70 kg [28].

The parameterization of the final model is given in Table 3. The table also includes results from a non-parametric bootstrap analysis with 1000 samples (nine runs failed to minimize and were excluded). Basic goodness-of-fit plots, a visual predictive check, the NONMEM control stream, and the observed data with individual fits are shown in Figures S3–S6 in the supplemental information. In Figure 2, we give the simulated PK profile for a hypothetical 70 kg individual with 90% confidence bands from 500 simulations along with the observed points from all volunteers in this study. The comparison of several secondary PK parameters of observed and simulated data (from 500 simulations, Table 4) shows the model to be in good agreement with the data obtained from the study.

Table 3

Final parameter estimates and results of a non-parametric bootstrap analysis (1000 runs)

	Estimate (% RSE)	Bootstrap analysis	
		Median	95% CI
Fixed Effects			
CL/F, l h^{-1}	7.67 (6.7)	7.65	6.64–8.77
V_c/F, l	89.13 (24.6)	90.62	44.45–122.06
V_p/F, l	234.30 (9.2)	234.18	200.69–291.55
Q/F, l h^{-1}	19.0 (13.8)	18.58	14.76–23.82
k_a, h^{-1}	0.55 (30.8)	0.55	0.31–0.89
NN	6 (fixed)		
MTT, h	1.05 (18.8)	1.04	0.76–1.46
Ratio DBS:Plasma	0.71 (1.6)	0.71	0.69–0.73
Interindividual Variability (ω)			
CL/F	0.25 (16.4)	0.24	0.14–0.32
V_c/F	0.10 (37.9)	0.11	0.01–0.25
V_p/F	0.20 (37.2)	0.2	0.05–0.31
Q/F	0.41 (23.5)	0.38	0.19–0.54
MTT	0.60 (19.1)	0.6	0.38–0.84
Residual Errors (σ)			
$Prop_{Plasma}$	0.09 (9.5)	0.09	0.08–0.11
$Prop_{DBS}$	0.11 (10.4)	0.07	0.04–0.09
Correlation $Prop_{Plasma}$ ~ $Prop_{DBS}$	0.41 (19.2)	0.41	0.16–0.57
Additive, ng ml^{-1}	0.71 (35.3)	0.67	0.23–1.04

CI, confidence interval; CL/F, clearance; MTT, mean transit time; NN, number of transit compartments; $Prop_{Plasma}$, proportional error in plasma; $Prop_{DBS}$, proportional error in dried blood spots (DBS); Q/F, intercompartmental transfer; % RSE, relative standard error [%RSE = 100 * (standard error/parameter estimate)]; V_c/F, central volume of distribution; V_p/F, peripheral volume of distribution

Discussion

This study provides a population PK model of oral ivermectin in healthy volunteers in plasma as well as DBS. The diagnostic criteria show that the final model adequately explains the observed data, and that no systematic biases exist. The model could be used to explore different dosing regimens through simulation, and would allow for estimation of DBS concentrations in field trials, an application that will become more and more important as ivermectin is being repurposed for new indications in MDAs. However, the ivermectin concentrations are lower in DBS than in plasma as ivermectin

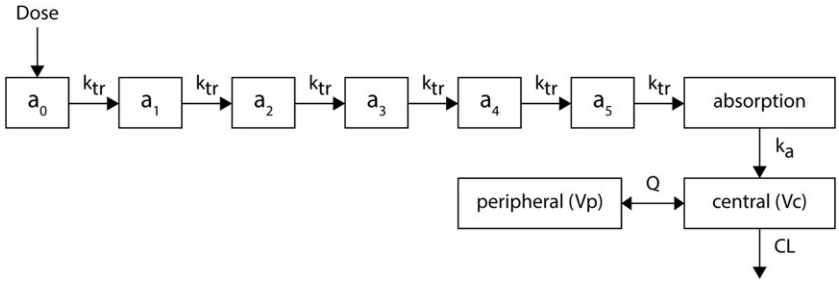

Figure 1

Overview of the final structural model

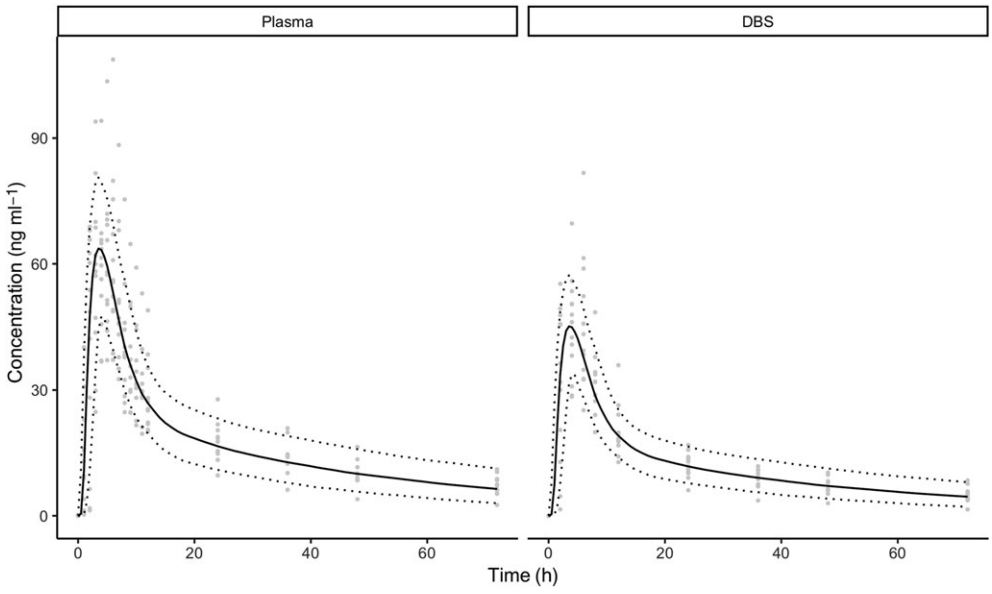

Figure 2

Simulated concentration curve over 72 h for a hypothetical typical individual with a weight of 70 kg (solid line) together with the observed data from all volunteers enrolled in the study (dots), and confidence lines at 5% and 90% from 500 simulated volunteers (dashed lines)

Table 4

Secondary pharmacokinetic parameters for observed data compared to simulation with the final population model (500 samples)

	Observed		Simulated	
	Mean	SD	Mean	SD
T_{max}, h	4.4	1.4	4.1	1.2
C_{max}, ng ml^{-1}	70.7	16.1	70.1	12.5
$AUC_{0-\infty}$, ng ml^{-1} h^{-1}	1743.5	602.5	1660.0	484.1
T_{half}, h	38.9	20.8	35.8	24.0
Vz/F, l h^{-1}	382.6	106.1	371.5	115.9
CL/F, l h^{-1}	7.7	2.8	7.8	2.2

$AUC_{0-\infty}$, area under the curve from zero to infinity with extrapolation of the terminal phase; CL/F, apparent clearance during terminal phase; C_{max}, peak concentration; SD, standard deviation; T_{max}, time of peak concentration; T_{half}, elimination half-life; Vz/F, apparent volume of distribution during terminal phase

only marginally diffuses into the red blood cells. Thus, DBS concentrations have to be adjusted by the hematocrit and the partition of the drug between plasma and red blood cells to estimate levels in plasma [29]. Our analysis reflects this through the use of a common correction factor (Ratio DBS: plasma). Interestingly, there was no improvement in the model fit when we introduced individual hematocrits as a covariate, maybe due to the fact that the study population covered only a limited, normal range of hematocrit values (Table 1). This indicates that hematocrit corrections are not necessary in order to interpret DBS samples in such subjects. Future studies using DBS that include subjects with hematocrits outside this range (e.g., anaemic patients), however, may need to account for this. Additionally, there may be variations in infants, children or elderly individuals, who were not examined in this trial, but who would be part of mass drug administrations. If an adjustment should become necessary in certain populations, there are a number of publications that validated adjustments of concentrations obtained from DBS by covariates such as, for example, hematocrit or protein binding [29–31].

We explored different approaches to understand the variability in PK. Although individual PK profiles appeared to be multiphasic, this could not be captured with the introduction of gallbladder filling and emptying into the model. As most of the peaks appeared well before the scheduled lunch time of 5 h post-dose (Figure S6), this could be attributed to differences in gastric emptying. The VPCs (Figure S4) further illustrate the difficulties with capturing peak concentrations in some individuals, although the sampling schedule was rich during the first 12 h post-dose and several approaches to modelling absorption and EHC were explored. Increasing the number of sampling points during the absorption phase could be helpful to characterize this better in future trials.

Individuals receiving ivermectin in resource-poor communities may suffer from malnutrition or other concomitant conditions. It could be assumed that lower amounts of fatty tissue such as in malnourished patients could affect the distribution, especially into deeper compartments. For these reasons, we recorded different physiological markers of nutrition such as BF%, TBW and serum albumin. These did not prove to be informative in the modelling process, which may be owing to the rather homogeneous and small trial population. Only total body weight showed any influence (on CL/F and V_c/F). Interestingly enough, despite ivermectin being a highly lipophilic drug, we found no covariate effects of body fat markers. Caution is of course advised when extrapolating, for example, to paediatric weight ranges to

simulate exposure in children as part of an MDA. Factors not considered in this trial like organ maturation, changes in enzyme and transporter activity, and other physiological changes during infancy and adolescence could have considerable impact on PK and also PD.

Finally, although P-gp is known to promote efflux of ivermectin, there was no appreciable effect on PK when the MDR1 3435C>T genotype was introduced into the model. Given the small sample size, it is likely the study was not sufficiently powered to detect effects from this single nucleotide polymorphism (SNP). It is, of course, also conceivable that other SNPs of MDR1 are more relevant for PK than 3435C>T. Other pharmacogenetic aspects such as CYP3A5 polymorphisms could influence PK of ivermectin [16], and this would be valuable to characterize in the target population of ivermectin MDAs in particular. We chose not to test for these as the focus of this study was on enterohepatic circulation, for which we assumed transporters located in the gallbladder, such as P-gp, were more important.

The two other previously published population-based analyses of oral ivermectin PK reported similar, albeit somewhat higher, values for CL/F and Vc/F (9.0 and 12.3 l h^{-1}, and 115 and 190 l, respectively) in adult healthy volunteers [10, 11]. This would be expected to give overall shorter elimination half-lives and lower peak concentrations as compared to our data. Mean elimination half-lives reported in literature following single oral doses of 200 μg kg^{-1} ivermectin range from 25 to 80.6 h, placing our estimate at the upper end [11, 32, 33]. The mean peak concentrations in these studies, whose weight-based dose is comparable to the mean dose of 181 μg kg^{-1} in our fixed-dose regimen, were consistently lower (43.2–50.1 ng ml^{-1}). We assume this is due to the fed state dosing in this trial, as food effect is described for ivermectin and the volunteers in the other trials mentioned were dosed in a fasted state [34].

Overall, this is the first published population-based analysis of ivermectin based on a trial specifically designed for this purpose. The population pharmacokinetic profile of oral ivermectin was influenced by subjects' weight. It provides robust estimates of the pharmacokinetics of oral ivermectin which can inform the ongoing and future efforts to repurpose ivermectin in neglected tropical diseases and support dose finding. Furthermore, we were able to show that DBS concentrations correlate strongly with plasma concentrations, and that DBS sampling could therefore be used in settings where peripheral venous sampling is impractical or not economical (e.g. in children or in field studies). This will help in designing sampling schedules for field studies with DBS. Despite all this, we would like to stress the homogeneity of the healthy young volunteers enrolled in this trial as the primary limitation of our model. Further trials are needed in the respective target populations, for instance children or malnourished individuals, to validate the approach more thoroughly.

Competing interests

This work was supported by the Forschungsfonds zur Förderung exzellenter Nachwuchsforschender (University of Basel, Switzerland) to F.H.; and the Science Pool of the University Hospital Basel, Switzerland, to F.H.

We thank Claudia Bläsi for study coordination and management, Beatrice Vetter for sampling and analysis, Emilie Müller and Patrick Simon for data monitoring, and CAMAG AG (Muttenz, Switzerland) for providing the DBS-MS 500 autosampler.

Contributors

The authors confirm that the Principal Investigator for this paper is S.K. and that he had direct clinical responsibility for patients. U.D. and C.S. contributed equally to this work.

References

1 Chaccour C, Hammann F, Rabinovich NR. Ivermectin to reduce malaria transmission I. Pharmacokinetic and pharmacodynamic considerations regarding efficacy and safety. Malar J 2017; 16: 161.

2 Menez C, Sutra JF, Prichard R, Lespine A. Relative neurotoxicity of ivermectin and moxidectin in Mdr1ab (−/−) mice and effects on mammalian GABA(A) channel activity. PLoS Negl Trop Dis 2012; 6: e1883.

3 Ejere HO, Schwartz E, Wormald R, Evans JR. Ivermectin for onchocercal eye disease (river blindness). Cochrane Database Syst Rev 2012; 8: CD002219.

4 Mectizan Donation Program. Annual highlights 2015. Available at https://mectizan.org/wp-content/uploads/2017/03/MDP_AnnHigh2015_Design-041516FINAL2-1.pdf (last accessed 6 June 2018).

5 Romani L, Whitfeld MJ, Koroivueta J, Kama M, Wand H, Tikoduadua L, *et al*. Mass drug administration for scabies control in a population with endemic disease. N Engl J Med 2015; 373: 2305–13.

6 PhRMA. Biopharmaceutical Research & Development: The Process Behind New Medicines 2015. Available at http://phrmadocs.phrma.org/sites/default/files/pdf/rd_brochure.pdf (last accessed 30 June 2018).

7 Gonzalez Canga A, Sahagun Prieto AM, Diez Liebana MJ, Fernandez Martinez N, Sierra Vega M, Garcia Vieitez JJ. The pharmacokinetics and interactions of ivermectin in humans – a mini-review. AAPS J 2008; 10: 42–6.

8 Fink DW, Porras AG. Pharmacokinetics of ivermectin in animals and humans. In: Ivermectin and Abamectin, ed Campbell WC. New York: Springer-Verlag, 1989; 113–30.

9 Krishna DR, Klotz U. Determination of ivermectin in human plasma by high-performance liquid chromatography. Arzneimittelforschung 1993; 43: 609–11.

10 El-Tahtawy A, Glue P, Andrews EN, Mardekian J, Amsden GW, Knirsch CA. The effect of azithromycin on ivermectin pharmacokinetics – a population pharmacokinetic model analysis. PLoS Negl Trop Dis 2008; 2: e236.

11 Kobylinski KC, Ubalee R, Ponlawat A, Nitatsukprasert C, Phasomkulsolsil S, Wattanakul T, *et al*. Ivermectin susceptibility and sporontocidal effect in Greater Mekong Subregion Anopheles. Malar J 2017; 16: 280.

12 Na-Bangchang K, Kietinun S, Pawa KK, Hanpitakpong W, Na-Bangchang C, Lazdins J. Assessments of pharmacokinetic drug interactions and tolerability of albendazole, praziquantel

and ivermectin combinations. Trans R Soc Trop Med Hyg 2006; 100: 335–45.

13 Dodds WJ, Groh WJ, Darweesh RM, Lawson TL, Kishk SM, Kern MK. Sonographic measurement of gallbladder volume. Am J Roentgenol 1985; 145: 1009–11.

14 Hricak H, Lieto RP. Sonographic determination of renal volume. Radiology 1983; 148: 311–2.

15 Kitajima K, Taboury J, Boleslawski E, Savier E, Vaillant JC, Hannoun L. Sonographic preoperative assessment of liver volume before major liver resection. Gastroenterol Clin Biol 2008; 32: 382–9.

16 Kudzi W, Dodoo AN, Mills JJ. Genetic polymorphisms in MDR1, CYP3A4 and CYP3A5 genes in a Ghanaian population: a plausible explanation for altered metabolism of ivermectin in humans? BMC Med Genet 2010; 11: 111.

17 Stieger B, Meier PJ. Pharmacogenetics of drug transporters in the enterohepatic circulation. Pharmacogenomics 2011; 12: 611–31.

18 Durnin JV, Womersley J. Body fat assessed from total body density and its estimation from skinfold thickness: measurements on 481 men and women aged from 16 to 72 years. Br J Nutr 1974; 32: 77–97.

19 Siri WE. Body composition from fluid spaces and density: analysis of methods, 1961. Nutrition 1993; 9: 480–91 discussion: 492.

20 Jonsson EN, Karlsson MO. Xpose – an S-PLUS based population pharmacokinetic/pharmacodynamic model building aid for NONMEM. Comput Methods Programs Biomed 1999; 58: 51–64.

21 Lindbom L, Ribbing J, Jonsson EN. Perl-speaks-NONMEM (PsN) – a Perl module for NONMEM related programming. Comput Methods Programs Biomed 2004; 75: 85–94.

22 Okour M, Brundage RC. Modeling enterohepatic circulation. Curr Pharmacol Rep 2017; 3: 12.

23 Harding SD, Sharman JL, Faccenda E, Southan C, Pawson AJ, Ireland S, *et al*. The IUPHAR/BPS Guide to PHARMACOLOGY in 2018: updates and expansion to encompass the new guide to IMMUNOPHARMACOLOGY. Nucleic Acids Res 2018; 46: D1091–106.

24 Alexander SPH, Kelly E, Marrion NV, Peters JA, Faccenda E, Harding SD, *et al*. The Concise Guide to PHARMACOLOGY 2017/18: Transporters. Br J Pharmacol 2017; 174 (Suppl. 1): S360–446.

25 Merck BV. Stromectol® Product Information. 2009.

26 European Medicines Agency Guideline on bioanalytical method validation 2015. Available at http://www.ema.europa.eu/docs/en_GB/document_library/Scientific_guideline/2011/08/WC500109686.pdf (last accessed 1 February 2018).

27 Savic RM, Jonker DM, Kerbusch T, Karlsson MO. Implementation of a transit compartment model for describing drug absorption in pharmacokinetic studies. J Pharmacokinet Pharmacodyn 2007; 34: 711–26.

28 Holford NH. A size standard for pharmacokinetics. Clin Pharmacokinet 1996; 30: 329–32.

29 Li W, Tse FL. Dried blood spot sampling in combination with LC-MS/MS for quantitative analysis of small molecules. Biomed Chromatogr 2010; 24: 49–65.

30 Duthaler U, Berger B, Erb S, Battegay M, Letang E, Gaugler S, *et al*. Using dried blood spots to facilitate therapeutic drug monitoring of antiretroviral drugs in resource-poor regions. J Antimicrob Chemother 2018; 73: 2729–37.

31 Jager NG, Rosing H, Schellens JH, Beijnen JH, Linn SC. Use of dried blood spots for the determination of serum concentrations of tamoxifen and endoxifen. Breast Cancer Res Treat 2014; 146: 137–44.

32 Amsden GW, Gregory TB, Michalak CA, Glue P, Knirsch CA. Pharmacokinetics of azithromycin and the combination of ivermectin and albendazole when administered alone and concurrently in healthy volunteers. Am J Trop Med Hyg 2007; 76: 1153–7.

33 Munoz J, Ballester MR, Antonijoan RM, Gich I, Rodriguez M, Colli E, *et al*. Safety and pharmacokinetic profile of fixed-dose ivermectin with an innovative 18 mg tablet in healthy adult volunteers. PLoS Negl Trop Dis 2018; 12: e0006020.

34 Guzzo CA, Furtek CI, Porras AG, Chen C, Tipping R, Clineschmidt CM, *et al*. Safety, tolerability, and pharmacokinetics of escalating high doses of ivermectin in healthy adult subjects. J Clin Pharmacol 2002; 42: 1122–33.

Supporting Information

Additional supporting information may be found online in the Supporting Information section at the end of the article.

http://onlinelibrary.wiley.com/doi/10.1111/bcp.13840/suppinfo

Figure S1 Bland–Altman plot of ivermectin measured in plasma and dried blood spot (DBS) samples (percent difference versus mean concentrations). The dashed line illustrates the mean percent difference of plasma compared to DBS. The white area defines the 95% limits of agreement. Gray dots correspond to observed values

Figure S2 Linear correlation (blue line) between concentrations found in plasma and dried blood spots (DBS). The linear regression model is $Concentration_{DBS} = -0.74 + Concentration_{plasma} * 0.753$ ($R^2 = 0.97$)

Figure S3 Goodness-of-fit plots for the final model (dashed lines: local weighted smooth). (A) Observed data *vs*. population predictions, (B) observed data *vs*. individual predictions, (C) absolute conditional weighted residuals (CWRES) *vs*. individual predictions, and (D) CWRES over time

Figure S4 Visual predictive check

Figure S5 NONMEM control stream of the final model

Figure S6 Individual plasma profiles (dots) and predictions [dashed: population (PRED); continuous: individual (IPRED)]